SEPARATION OF SIGNALS DUE TO ARTERIAL
AND VENOUS BLOODFLOW, IN THE DOPPLER
SYSTEM, THAT USES CONTINUOUS ULTRASOUND

by

W.P. Goes

Group Measurement and Control
Department of Electrical Engineering
Eindhoven University of Technology
Eindhoven, The Netherlands

SEPARATION OF SIGNALS DUE TO ARTERIAL AND VENOUS
BLOODFLOW, IN THE DOPPLER SYSTEM, THAT USES
CONTINUOUS ULTRASOUND

by

W.P. Goes

TH-Report 73-E-40

June 1973

SEPARATION OF SIGNALS DUE TO ARTERIAL AND VENOUS BLOODFLOW,
IN THE DOPPLER SYSTEM, THAT USES CONTINUOUS ULTRASOUND

W.P. Goes

Eindhoven University of Technology

Department of Electrical Engineering

Eindhoven, Netherlands

Summary.

The received signal of a doppler flowmeter using continuous
ultrasound may contain positive and negative frequency shifts.
In many cases positive frequency shifts can be related to
arterial blood flow, while negative shifts are related to
venous flow. However if the arterial flow becomes negative
during the cardiac cycle, this is true to a certain extent.
This report deals with a simple solution to separate the
positive and negative spectra of the doppler signal. The
determination of the average frequency of the positive and
negative spectra is done in a well known way (ref. 1,
Appendix A). However, in order to make the interpretation
of the registrations easier, a multiplicand, depending upon
the ratio of the powers of positive and negative spectra, is
added.

Contents.

1. Introduction.

Measuring the blood flow in arteries and veins by means of ultrasound using the doppler frequency shift principle is a method which is harmless and confortable to the patient. This is one of the main reasons why many technicians exert themselves to the utmost to design apparatus that can derive this flow from the received doppler signals.

If one knows the cross-section of the vessel and the average velocity of the blood in this cross-section, the flow is given by the product of these. Flow, cross-section and average velocity are time-dependent.

Determination of the cross-section is possible by means of pulsed ultrasound echoing, but this problem will not be dealt with in this report. The average velocity can be measured using continuous ultrasound.

The principle that underlies this velocity measurement is as follows (fig. 1). A beam of ultrasound, generated by a piezo-electrical transducer, which is in resonance, is sent in the direction of the blood vessel. Moving particles, which are suspended in the blood, (erytrocytes) scatter the ultrasound in all directions. Because of the motion of the particles, the original frequency of the ultrasound is changed.

This frequency change is dependent upon the original frequency, the velocity of the particle and upon the direction in which the sound is scattered. A small amount of this scattered sound excites the receiving transducer, which converts this mechanical signal into an electrical one. The radial frequency shift, with respect to the radial frequency of the transmitted signal can be expressed as:

$$\Delta\omega = \omega - \omega_o = \frac{\omega_o}{c} \cdot v \cdot \left(\cos \alpha + \cos \beta \right) \qquad \text{(ref. 1)} \quad (1)$$

(for the definition of the characters, see the list of symbols at page 25).

Because of the velocity profile in the bloodvessel, the
particles have different velocities and the received signal
contains a spectrum of radial frequencies. A well known way
to process the received signal in order to get an output
proportional to the average blood velocity, is the zero-
crossing method, which is cheap and reliable from the point
of view of instrumentation. However this method results in
a calibration factor dependent on the velocity profile.

An elegant solution is given by ir. Arts (ref. 1), who makes
use of analogue computing techniques to calculate the
average radial frequency shift as given by the expression:

$$\Delta\omega_{average} = \frac{\int_{\Delta\omega_{min}}^{\Delta\omega_{max}} \Delta\omega . \ \Phi(\Delta\omega) . \ d(\Delta\omega)}{\int_{\Delta\omega_{min}}^{\Delta\omega_{max}} \Phi(\Delta\omega) . d(\Delta\omega)} \qquad (2)$$

In his report he proves that the average frequency shift
is proportional to average blood velocity, independent of
the velocity profile.

All moving particles, which are in the cross-volume of the
transmitter and receiver beam contribute to the signal at the
input of the receiver. This means that only the bloodvessel
of which the flow has to be measured may be in this cross-
volume. This condition cannot be fulfilled in all cases,
which has two reasons:
a) The surface of the transducers is a semicircle with a
   radius of some five mm. This means that the volume of
   intersection of the transmitter and receiver beam is
   quite large.
b) In many cases, especially in the limbs, arteries are
   flanked by veins.

If the wanted bloodvessel cannot be "picked out" by positioning
the transducers, much can be done in an electronical way. Then,
use is made of the fact that generally the flow of blood in

artery and vein has opposite directions, thus causing opposite frequency shifts.

In this report a method is described to separate these opposed frequency shifts. Some difficulties arise if the direction of arterial blood flow changes sign during the cardiac cycle. In that case separation of positive and negative frequency shifts does not correspond to the separation of arterial and venous flow. In order to make the reading of the results in this case easier, a multiplicand is introduced.

2. General theoretical considerations.

The receiving transducer cannot distinguish between the signals of arteries and those of veins. Thus, schematically, all vessels, in parallel, in the cross-volume of transmitter and receiver beam can be regarded as being just one (fig. 2).

In reference 1 it is proved that in certain conditions the average radial frequency-shift is related to the average velocity as:

$$\Delta \omega_{av} = \frac{\omega_o}{c} \left(\cos \alpha + \cos \beta \right) . V_{av} \tag{3}$$

in which:

$$V_{av} = \frac{1}{N} \sum_{i=1}^{N} v_i \tag{4}$$

The electronic equipment built by Arts and tested by Weys (ref. 3) determines the average radial frequency shift, given by equation (3). This means that if one is interested in the velocity of the blood in an artery, the output of the apparatus may be influenced by the velocity of the blood in a vein (fig.3). The processing of the signal in this situation (simplified, as only two frequency components are assumed) is given in appendix A. If $A \neq 0$ (equation 18), which means that there is a venous flow, the output is not equal to ω_{d2}, which is caused by the arterial flow.

Equation (4) can be separated into four parts:

$$V_{av_t} = \frac{1}{N_t} \left\{ \sum_{i=1}^{N_{a+}} v_i + \sum_{j=1}^{N_{a-}} v_j + \sum_{k=1}^{N_{v+}} v_k + \sum_{\ell=1}^{N_{v-}} v_\ell \right\} \tag{5}$$

in which

$$N_t = N_{a+} + N_{a-} + N_{v+} + N_{v-}$$

We are interested in the value of

$$V_{av.a} = \frac{1}{N_{a+} + N_{a-}} \left\{ \sum_{i=1}^{N_{a+}} v_i + \sum_{j=1}^{N_{a-}} v_j \right\} \tag{6}$$

which can be achieved by the apparatus of Arts, only if
N_{v+} as well as N_{v-} in (5) are zero.

Separation of upper and lower frequency spectra gives a
way to separate some terms of equation (5). If this is done
and the average radial frequency of each spectrum is
determined in the way described in appendix A, the measured
average velocity becomes:

$$V_{av+} = \frac{1}{N_{a+} + N_{v+}} \left\{ \sum_{i=1}^{N_{a+}} v_i + \sum_{k=1}^{N_{v+}} v_k \right\} \tag{7a}$$

$$V_{av-} = \frac{1}{N_{a-} + N_{v-}} \left\{ \sum_{j=1}^{N_{a-}} v_j + \sum_{\ell=1}^{N_{v-}} v_\ell \right\} \tag{7b}$$

If N_{v+} and N_{a-} are zero at any time, the average velocities
of arterial (7a) and venous (7b) flow are obtained (fig. 4).
Normally the flow in a vein is always negative and moreover
stationary, so $N_{v+} = 0$, $N_{v-} = N_v$.

In peripheral arteries the flow is always positive, so N_{a-}
will be zero at any time too. In these cases the discrimination
between aterial and venous velocities can be acheived by
separation of the upper and lower spectra.

However there are also arteries (e.g. aorta) which have a
negative flow during a part of the cardiac cycle. For such a
situation the discrinination between arterial and venous
velocities cannot be made as described before.

To analyse this situation, we have to split up a period of
the cardiac cycle into two parts:

-T_1, the time that the arterial flow is positive.

-T_2, the time that this flow is negative.

The assumption that changing the direction of the flow in an artery includes zero velocity of all particles at the same moment results in: (fig. 5)

a) during T_1; $N_{a+} = N_a$ and $N_{a-} = 0$. Expression (7) can be simplified to:

$$V_{av+} = V_{a+} = \frac{1}{N_a} \sum_{i=1}^{N_a} v_i$$

$$V_{av-} = V_{v-} = \frac{1}{N_v} \sum_{\ell=1}^{N_v} v_\ell \qquad (8a)$$

b) during T_2; $N_{a+} = 0$ and $N_{a-} = N_a$. Expression (7) can be simplified to:

$$V_{av+} = V_{a+} = 0$$

$$V_{av-} = V_{a-}' + V_{v-}' = \frac{1}{N_a + N_v} \sum_{j=1}^{N_a} v_j + \frac{1}{N_a + N_v} \sum_{\ell=1}^{N_v} v_\ell \qquad (8b)$$

These measured values V_{av+} and V_{av-} may vary during the cardiac cycle, as given in fig. 6. From formula (8a) it is clear that during the period T_1, when arterial flow is positive, the system determines the real average velocities, present in artery and vein. However expression (8b) shows that during the period T_2 the measured average velocity in the artery V_{a-}' (the time dependent part of V_{av-} in fig. 6) as well as the measured average velocity in the vein V_{v-}', is too low. The measured values need a correction multiplicand $(N_a + N_v)/N_a$ resp. $(N_a + N_v)/N_v$ in this period in order to get the real average velocities:

$$V_{a-} = \frac{1}{N_a} \sum_{j=1}^{N_a} v_j \quad , \quad V_{v-} = \frac{1}{N_v} \sum_{\ell=1}^{N_v} v_\ell$$

As the interpretation of a registration as given in fig. 6 is difficult and moreover a system that needs a correction multiplic and during a certain time T_2 is inelegant, the averaging system is changed in such a way that the measured values during the whole cardiac cycle are:

$$V'_{av+} = V'_{a+} = \frac{1}{N_a + N_v} \sum_{i=1}^{N_a} v_i$$

$$V'_{av-} = \frac{1}{N_a + N_v} \sum_{j=1}^{N_a} v_j + \frac{1}{N_a + N_v} \sum_{l=1}^{N_v} v_l$$

(9)

A probable output of such a system is given in fig. 7. In the following chapters a description is given of a system in which:

a) The upper and lower doppler spectra are separated.

b) The values V'_{av+} and V'_{av-} are determined.

3. Separation of the positive and negative spectra.

This separation can be done in three different ways, i.e.

a) By use of two bandpass filters, which have their pass-
   band on opposite sides of f_o (fig. 8a).
   In order to get a reasonable separation of the channels
   the roll-off at frequency $f_o \pm f_{min}$ must be very
   precipitous, which is hardly achievable for the given
   values of f_o and f_{min}. Moreover the frequency f_o,
   which depends upon the resonance frequency of the
   transducers, may not be changed in such a system. The
   generator, that drives the transducer must be stable
   at 10^{-5}.
   $(f_o = 5 \times 10^6 \text{ hz} \longrightarrow \Delta f = 10^{-5} \times 5 \times 10^6 \text{ hz} = 50 \text{ hz})$.

b) By use of an intermediate mixing frequency and bandpass
   filtering at a lower frequency level (fig. 8b).
   In this case the received signal is mixed with a signal
   of a frequency $f_o + f_{int}$ (f_{int} is about 20 kHz). The
   lower sideband of the mixed signal passes through two
   bandpass filters. The result is a separation of the two
   spectra. Another mixing with a signal of the intermediate
   frequency is necessary to shift each sideband from around
   $f = f_{int}$ to $f = 0$.
   This system does not make high demands upon the bandpass
   filters, which can now be designed on opposite sides of
   the intermediate frequency. However the penalty is the
   need for an extra step of demodulation, two bandpass
   filters and an extra signal generator of relatively low
   stability (2.5×10^{-3}).

c) By use of an active phase shifting network.
   This method which is used in the final apparatus will
   be explained more in detail in paragraph 3.1.

3.1. Demodulation and separation of the two spectra of the doppler signal by the phase-shifting method

Figure 9 shows a simplified block-diagram of the system.
Its operation will be explained with the help of the signal

$$S_h(t) = A \cos(\omega_o - \omega_{d1})t + B \cos(\omega_o + \omega_{d2})t$$

The first term is due to particles moving in the negative direction, the second part arises from particles moving in the opposite direction. Demodulation of the signal by $C \cos(\omega_o t + Q)$ and $C \cos(\omega_o t + \varphi + \Delta\varphi)$ respectively gives:

$$S_{d1}' = \frac{AC}{2} \left\{ \cos((2\omega_o - \omega_{d1})t + \varphi) + \cos(-\omega_{d1}t - \varphi) \right\} +$$

$$+ \frac{BC}{2} \left\{ \cos((2\omega_o + \omega_{d2})t + \varphi) + \cos(\omega_{d2}t - \varphi) \right\}.$$

$$S_{d2}' = \frac{AC}{2} \left\{ \sin((2\omega_o - \omega_{d1})t + \varphi + \Delta\varphi) - \sin(-\omega_{d1}t - \varphi - \Delta\varphi) \right\} +$$

$$+ \frac{BC}{2} \left\{ \sin((2\omega_o + \omega_{d2})t + \varphi + \Delta\varphi) - \sin(\omega_{d2}t - \varphi - \Delta\varphi) \right\}$$

Low-pass filters suppress the unwanted modulation products, thus

$$S_{d1} = \frac{AC}{2} \cos(\omega_{d1}t + \varphi) + \frac{BC}{2} \cos(\omega_{d2}t - \varphi).$$

$$S_{d2} = \frac{AC}{2} \sin(\omega_{d1}t + \varphi + \Delta\varphi) - \frac{BC}{2} \sin(\omega_{d2}t - \varphi - \Delta\varphi).$$

These signals are subjected to circuits that give a phase shift of γ and δ radians over a defined frequency range. This results in

$$S_{ps\,\gamma} = \frac{AC}{2} \cos(\omega_{d1}t + \varphi - \gamma) + \frac{BC}{2} \cos(\omega_{d2}t - \varphi - \gamma)$$

$$S_{ps\,\delta} = \frac{AC}{2} \sin(\omega_{d1}t + \varphi + \Delta\varphi - \delta) - \frac{BC}{2} \sin(\omega_{d2}t - \varphi - \Delta\varphi - \delta)$$

In order to obtain the separated spectra, these signals are added and subtracted.

$$S_a = S_{p a \gamma} + S_{p \epsilon \delta} = \frac{AC}{2} \left\{ \sin\left(\omega_{d_1} t + \varphi - \gamma + \frac{\pi}{2}\right) + \sin\left(\omega_{d_1} t + \varphi + \Delta\varphi - \delta\right) \right\} +$$

$$+ \frac{BC}{2} \left\{ \sin\left(\omega_{d_2} t - \varphi - \gamma + \frac{\pi}{2}\right) - \sin\left(\omega_{d_2} t - \varphi - \Delta\varphi - \delta\right) \right\}$$

$$= AC \left\{ \cos \frac{-\gamma + \frac{\pi}{2} - \Delta\varphi + \delta}{2} \cdot \sin\left(\omega_{d_1} t + \varphi + \frac{-\gamma + \frac{\pi}{2} + \Delta\varphi - \delta}{2}\right) \right\} +$$

$$+ BC \left\{ \sin \frac{-\gamma + \frac{\pi}{2} + \Delta\varphi + \delta}{2} \cdot \cos\left(\omega_{d_2} t - \varphi + \frac{-\gamma + \frac{\pi}{2} - \Delta\varphi - \delta}{2}\right) \right\}.$$

similar:

$$S_s = AC \left\{ \sin \frac{-\gamma + \frac{\pi}{2} - \Delta\varphi + \delta}{2} \cdot \cos\left(\omega_{d_1} t + \varphi + \frac{-\gamma + \frac{\pi}{2} + \Delta\varphi - \delta}{2}\right) \right\} +$$

$$+ BC \left\{ \cos \frac{-\gamma + \frac{\pi}{2} + \Delta\varphi + \delta}{2} \cdot \sin\left(\omega_{d_2} t - \varphi + \frac{-\gamma + \frac{\pi}{2} - \Delta\varphi - \delta}{2}\right) \right\}.$$

For $\delta - \gamma = \frac{\pi}{2} + \Delta\Psi$ we find:

$$S_a = AC \cos\left(\frac{\pi}{2} + \frac{-\Delta\varphi + \Delta\Psi}{2}\right) \cdot \sin\left(\omega_{d_1} t + \varphi + \frac{-2\gamma - \Delta\Psi + \Delta\varphi}{2}\right) +$$

$$+ BC \sin\left(\frac{\pi}{2} + \frac{\Delta\varphi + \Delta\Psi}{2}\right) \cdot \cos\left(\omega_{d_2} t - \varphi + \frac{-2\gamma - \Delta\varphi - \Delta\Psi}{2}\right).$$

$$S_s = AC \sin\left(\frac{\pi}{2} + \frac{-\Delta\varphi + \Delta\Psi}{2}\right) \cdot \cos\left(\omega_{d_1} t + \varphi + \frac{-2\gamma + \Delta\varphi - \Delta\Psi}{2}\right) +$$

$$+ BC \cos\left(\frac{\pi}{2} + \frac{\Delta\varphi + \Delta\Psi}{2}\right) \cdot \sin\left(\omega_{d_2} t - \varphi + \frac{-2\gamma + \Delta\varphi - \Delta\Psi}{2}\right).$$

If $\frac{\Delta\varphi + \Delta\Psi}{2} = \frac{-\Delta\varphi + \Delta\Psi}{2}$ then the expressions of S_a and S_s
can be reduced to:

$$S_a = BC \cos\left(\omega_{d_2} t - \varphi - \gamma\right) \tag{10}$$

$$S_s = AC \cos\left(\omega_{d_1} t + \varphi - \gamma\right) \tag{11}$$

The ultimate result is that the positive spectrum (ω_{d2})
appears at the output of the adder, and the negative spectrum
(ω_{d1}) at the output of the substrator.

Conditions to this are:

a) $\Delta\varphi$ as well as $\Delta\Psi$ must be zero. This means that the demodulating carriers must have a phase-shift of 90°

($\Delta\varphi$ = o).

The difference in phase-shift of the two networks must be 90° ($\Delta\Psi$ = o).

b) The phase-shift ($\delta - \gamma$) must be 90° for all the regarded frequencies.

c) The demodulating carriers must have equal amplitudes.

d) If filters are used in the two channels, their amplitude as well as their phase characteristics must be equal. Figure 10 illustrates the case that all these requirements are satisfied.

3.2. A figure of merit of the separation of the spectra.

If the two branches of the system, drawn in fig. 9 contain parts, which have different phase and/or amplitude characteristics there will be "cross-talk" in the separated spectra. A simple calculation, that can be explained from the diagram in fig. 11, gives some figures about the quality of separation.

The diagram shows the worst case of a doppler signal of just one (negative) frequency, S_{d1}. $S_{ps\gamma}$ is the signal of the upper branch of the system. The phase and amplitude of S_{d1} are used as references. Differences in amplification and phase shift in the corresponding parts of upper and lower branches are considered.

The total error of the phase ($\Delta\varphi_{tot}$) is the sum of errors of the demodulators, bandpass filters and phase shifting networks γ and δ. In the same way Δ amplitude$_{tot}$ is the result of errors in amplification factors of those circuits.

The amount of "cross-talk" is defined as: $C_t = \dfrac{S_a}{S_s} \times 100\%$.

The dependency of C_t on $\Delta\varphi_{tot}$ and Δ amplitude$_{tot}$ is given in fig. 12. This calculation is done in the case

that the signal contains just one frequency; in reality C_t is a function of the frequency. The output of the processing part of the system, determining the average frequencies of the spectra, appearing at the adder and the subtractor, is independent of the amplitude (power) of the signals (see apppendix A), so the separation of the channels must be perfect. In the case of having just positive doppler frequency shifts, a small "cross-talk" from the positive to the negative spectrum causes a considerable output voltage at the negative channel. The introduction of the multiplicand, which is dependent on the relative values of the powers of the negative and positive spectra bypasses this inconvenience.

Measurements of the two realised bandpass filters show a phase difference $\leqslant 1$ degree. The phase error after de-modulation is of the same order. Because of these values the circuits that provide the γ and δ phase-shifts are designed in such a way that the deviation of the desired value $(\delta - \gamma = \pi/2)$ is less than one degree.

3.3. The networks that give the phase-shift γ and δ.

The demands made upon the circuits , that provide the phase shift γ and δ are:
a) The difference $\delta - \gamma$ has to be 90°, as good as possible, in the desired frequency range.
b) The amplification must be constant in that frequency range.

The frequency shifts, which are in the doppler spectra, positive as well as negative, are dependent upon the velocities of the erytrocytes in the following way:

$$\Delta\omega = \omega - \omega_0 = \frac{\omega_0}{c} \cdot v \cdot \left(\cos\alpha + \cos\beta\right). \tag{12}$$

The used values are:

$$V_{max} = 1 m/sec, \quad f_0 \approx 5 \text{ MHz}, \quad 150° < \alpha = \beta > 120°$$

and

$$c = 1,5 \times 10^3 \text{ m/sec}.$$

The maximum frequency-shift and so the maximum frequency
in the demodulated signal is thus 6000 Hz. The moving arterial
walls, the cross-talk of the crystals and the reflections at
the surface of the skin introduce unwanted signals, which
limit the usable doppler spectrum to a lowest frequency of
150 hz.

A way to calculate the poles and zeros of a network that
gives a certain phase-shift is given by Prof.dr. J.J. Zaalberg
van Zelst (ref. 2). A method to achieve a phase-shift of 45°
with an accuracy better than 20' in the frequency range of
150 - 6000 hz irrespective of a constant amplitude charac-
teristic is given in appendix B.

We used the results of this calculation to evaluate two
networks which have a phase difference of 90 degrees and
constant amplitude characteristics.

The poles and zeros of the calculated network are at the
negative real axis of the complex frequency plane. In order
to achieve a constant amplification in the desired frequency
range we have to add poles and zeros on the positive real
axis (fig. 13a). This must be done in such a way that each
positive pole (zero) corresponds to a negative zero (pole).
The added poles and zeros on the positive real axis double
the phase-shift, which becomes 90°. The transfer function
of such a network becomes

$$H = H_o \prod_{K=1}^{3} \frac{1 + P_K \cdot P}{P + P_K} \cdot \frac{P - P_K}{1 - P_K \cdot P} \qquad \text{(see appendix B).} \qquad (13)$$

The poles on the positive real axis will introduce in-
stabilities in the circuit. This result shows that the
realisation of one stable circuit, giving a constant phase
shift of 90 degrees over the frequency range is impossible.
However this gives rise to another instrumentation method.

Starting from fig. 13a one might split up the poles and
zeros of formula (13) as shown in fig. 13b and fig. 13c.
The system represented by the zeros and poles in fig. 13b

is stable, has a constant amplification, and gives a phase shift $\delta(\omega)$. Fig. 13c represents an unstable system, having a constant amplification and a phase-shift $90° - \delta(\omega)$. Changing poles (zeros) to zeros (poles) in fig. 13c, results in a stable system (fig. 13d) with a constant amplification and a phase-shift $\delta(\omega) - 90° = \gamma(\omega)$. For a signal supplied to both inputs of the systems represented by fig. 13b and fig. 13d, the outputs will have a phase difference of 90°.

In order to check whether the calculated poles and zeros (appendix B) result in the desired phase-shift, their values are used as data to a computer program, that calculates this shift in the desired frequency range. The result is given in figure 14.

3.4. Implementation of the networks

A simple network, that has a negative pole and a positive zero on the real axis, symmetrical around the origin is a series connection of a capacitor and a resistor, which are fed with opposed voltages (fig. 15a). The actual hardware circuit implementation is given in fig. 15b. Three of these circuits are connected in series to perform the system of fig. 13b or fig. 13d; another one is added to achieve a low output impedance.

The result, $\delta - \gamma$, is measured and given in fig. 14. The deviation of this to the calculated value is due to the errors in the actual time constants, which have to be realised by selected resistors and capacitors. The result is:

$$\delta - \gamma = 90° \; {+ \, 55' \atop - \, 1° \, 28'}$$

which is slightly worse, than we expected.

4. The signal processing part of the system.

As derived before, the developed system has to measure:

$$V_{av+}' = \frac{1}{N_a + N_v} \sum_{i=1}^{N_a} v_i \tag{9}$$

$$V_{av-}' = \frac{1}{N_a + N_v} \left\{ \sum_{j=1}^{N_a} v_j + \sum_{l=1}^{N_v} v_l \right\}$$

The values V_{av+}' and V_{av-}' are time dependent. It can be seen that if the direction of arterial flow changes sign the value $1/(N_a + N_v) \sum_{i=1}^{N_a} v_i$ disappears from the one output (V_{av+}') and moves to the other output as $1/(N_a + N_v) \sum_{j=1}^{N_a} v_j$. Because of the fact that in the system the multiplicand $1/(N_a + N_v)$ is saved during this move, the outputs can be interpreted in a nicer way.

Equation (3) gives the relation between $\Delta\omega_{av}$ and V_{av}. By introducing the multiplicand $1/(N_a + N_v)$ the "average value " of each spectrum is now defined as:

$$\Delta\omega_{av}(+,-) = \frac{\displaystyle\int_0^{\Delta\omega_{max}(+,-)} \Delta\omega(+,-) \cdot \Phi(\Delta\omega,+,-) \, d(\Delta\omega)}{\displaystyle\int_0^{\Delta\omega_{max}(+)} \Phi(\Delta\omega,+) \, d(\Delta\omega) + \int_0^{\Delta\omega_{max}(-)} \Phi(\Delta\omega,-) \, d(\Delta\omega)} \tag{13}$$

A block-diagram of the system determining this value is given in fig. 16. The first part gives the demodulation and separation of the doppler sidebands. For this system we will analyse the processing of a signal that contains two frequency components, one in each sideband.

$$S_a = BC \cos\left(\omega_{d2} t - \varphi - \gamma\right) \tag{10}$$

$$S_s = AC \cos\left(\omega_{d1} t + \varphi - \gamma\right) \tag{11}$$

The signal of which the total power is derived is:

$$S_{d_1} = \frac{AC}{2} \cos(\omega_{d_1} t + \varphi) + \frac{BC}{2} \cos(\omega_{d_2} t - \varphi). \qquad (14)$$

Differentiation of the positive spectrum yields:

$$S_{dp} = -\omega_{d_2} \cdot BC \sin(\omega_{d_2} t - \varphi - \gamma)$$

The signal S_{d1} gets a phase-shift of δ radians, thus

$$S_K = \frac{AC}{2} \cos(\omega_{d_1} t + \varphi - \delta) + \frac{BC}{2} \cos(\omega_{d_2} t - \varphi - \delta)$$

The numerator of the divider in the positive channel is found by taking the D.C. component after the multiplication of S_{dp} and S_K.

$$S_{dp} \times S_K = -\omega_{d_2} \cdot \frac{ABC^2}{4} \left\{ \sin((\omega_{d_2} + \omega_{d_1})t - \gamma - \delta) + \sin((\omega_{d_2} - \omega_{d_1})t \right.$$

$$\left. -2\varphi - \gamma + \delta) \right\} - \omega_{d_2} \frac{B^2 C^2}{4} \left\{ \sin(2\omega_{d_2} t - \varphi - \gamma - \varphi - \delta) + \sin(\delta - \gamma) \right\}.$$

So for the numerator of the positive channel we find

$$N(+) = -\omega_{d_2} \frac{B^2 C^2}{4} \sin(\delta - \gamma) = -\omega_{d_2} \frac{B^2 C^2}{4}. \qquad (15)$$

The denominator of the divider is found by taking the D.C. component of the square of S_K:

$$S_K^2 = \frac{A^2 C^2}{8} \left\{ 1 - \cos 2(\omega_{d_1} t + \varphi - \delta) \right\} + \frac{B^2 C^2}{8} \left\{ 1 - \cos 2(\omega_{d_2} t - \varphi - \delta) \right\} +$$

$$+ \frac{ABC^2}{8} \left\{ \cos((\omega_{d_1} + \omega_{d_2})t - 2\delta) + \cos((\omega_{d_1} - \omega_{d_2})t + 2\varphi) \right\}.$$

$$D = \frac{A^2 C^2}{8} + \frac{B^2 C^2}{8}$$

This results in

$$V_{out}(+) = \frac{N(+)}{D} = -\frac{B^2}{A^2 + B^2} \cdot 2 \cdot \omega_{d_2} \qquad \# \frac{1}{N_a + N_v} \Sigma v_i \qquad (16)$$

similar

$$V_{out}(-) = \frac{N(-)}{D} = -\frac{A^2}{A^2 + B^2} \cdot 2 \cdot \omega_{d_1} \qquad \# \frac{1}{N_a + N_v} \left\{ \Sigma (v_j + v_k) \right\} \qquad (17)$$

5. Remarks on the electronic instrumentation and measuring equipment.

5.1. Electronic instrumentation.

A description of the main parts will be given with the help of fig. 16. The signal of the receiving transducer is amplified (L 103) and fed into the modulators (MC 1596). By means of passive RC circuits the modulating carriers are derived from the signal of the generator. Because of the frequency dependency of their amplitudes, these carrier signals have to be large enough to insure demodulation by means of h.f. switching, which is independent of those amplitudes. This is necessary to obtain a sufficient separation of the doppler sidebands (see chapter 3).

After demodulation, these signals are filtered by two band-pass filters, which have a passband of 320 - 10.000 hz (2 x µA 709) and a gain of 40 dB.

The active phase-shifting networks have been described extensively in chapter 3.3. The resulting signals are added and subtracted with the aid of two operational amplifiers (µA 709), which have a gain of 12 dB.

The gains of the active phase-shifting networks have such values that the amplitude of the spectrum of the denominator is twice the amplitude of the numerator. This is the most favourable ratio with respect to the signal processing part of the system. This part is described in detail by Weys in his report, to which we refer (ref. 3).

5.2. Measuring equipment.

In a test setup two bloodvessels are simulated by latex tubes, which have thin walls. One of these tubes is in a fixed position. the position of the other can be changed (fig. 17). The whole setup is placed in water to provide a medium, which has low acoustical losses between the transmitter (receiver)

crystal and the latex tubes. Small latex spheres of the
size of erytrocytes, suspended in water is an acceptable
simulator of blood. During the measurements the actual
flow is measured with an electromagnetic flowmeter.
(Transflow 600 - Skalar instruments.)

6. Measured results.

a) Calibration of the two channels.

An h.f. generator that can supply a very small voltage (some μV_{eff}) is connected to the input of the apparatus. The differential frequency between this generator and the one that provides the demodulating carriers is controlled so, as to obtain both doppler sidebands (fig. 18). The linearity of the system for one frequency at a time (V_{out} versus Δf) is nice and the sideband separation is sufficient up to 6000 hz.

b) Stationary flow in one vessel.

In this case the laminary flow produces a spectrum of frequencies. The output of the apparatus gives the real average frequency of this spectrum (fig. 19). A numerical check of the sensitivity is as follows:

$$\Delta\left(\Delta f_{av}\right)/\Delta v_{av} = \frac{f_o}{c}\left(\cos\alpha + \cos\beta\right) = \frac{5.14 \times 10^6}{1.5 \times 10^3}\left(.707 + .707\right) = 48.4 \ hz/cm/sec.$$

The diagram of fig. 18 gives $\Delta V_{out}/\Delta\left(\Delta f_{av}\right) = 2.3$ V/khz, thus theoretically

$$\Delta V_{out}/\Delta\left(\Delta f_{av}\right) \times \Delta\left(\Delta f_{av}\right)/\Delta v_{av} = \Delta V_{out}/\Delta v_{av} = .11 \ V/cm/sec.$$

The slope of the line in fig. 19 is .11 V/cm/sec. It should be noticed that this line does not cross the origin. This is a consequence of the bandpass filters. Because of the loss of the lowest frequencies, the measured value Δf_{av} is slightly more than the real Δf_{av}

c) Varying flow in one vessel.

If the direction of flow is made alternating, the output V_{av} jumps from the positive output to the negative one and vice versa (fig. 20).

d) Stationary flow in the vein, pulsatile flow in the artery.

The output of both channels is given in fig. 21. It can be seen that the contribution of arterial flow moves from the one output to the other and keeps the same scale. This is a result of the introduction of the multiplicand described in chapter 2 (equation 9).

e) The average velocity of the blood in the radial artery.

The transducers were placed upon the wrist in such a position that no signal was picked up from the adjacent vein (checked by the signal at the output of the subtractor). The velocity of the blood in the radial artery appeared to be positive during all the cardiac cycle (fig. 22).

7. Conclusions and suggestions.

In the realised system that uses continuous ultrasound to
determine momentaneously the average velocity of blood in
a bloodvessel, the signals, coming from two different
vessels can be separated under certain conditions.
Separation of the upper and lower sidebands and so
separation of positive and negative velocities, does not
correspond to separation of signals coming from artery
and vein. This is merely a separation in space.

If the received signal is caused by arterial as well as
venous flow, we can take advantage of the fact that in all
cases the bloodflow in a vein is stationary and has a
negative sign. The realised apparatus can be used to
position the crystals in such a way that no venous signals
are picked up. This can be done by controlling the murmer
that can be heard in a loudspeaker, connected to the output
of the subtractor. If there is no constant murmer left the
output is due to arterial flow. If this fails there remain
two possibilities:

a) The arterial bloodflow becomes positive and negative
   during the cardiac cycle.

   The output of the two channels cannot be used to
   calculate the flow in artery and vein. (flow = average
   velocity x cross-section.) For this case a special
   weighting factor is introduced to make the outputs useful
   for visual assessment of the bloodflow. If we compare
   equations $(16/17)$ and (18) we see that the output of the old
   system (Arts) is divided into two parts in our system
   (fig. 23).

   A suggestion to use the outputs to calculate the flow
   in the artery and the vein may be:

   The real velocity in the artery during T_1

$$\frac{N_a + N_v}{N_a} \cdot \frac{1}{N_a + N_v} \sum_{i=1}^{N_a} V_i \, .$$

   and

the velocity in the vein during T_1 is

$$\frac{N_a + N_v}{N_v} \cdot \frac{1}{N_a + N_v} \sum_{\ell=1}^{N_v} v_\ell$$

The cross-section of the artery is K_1 x N_a and the one of the vein K_2 x N_v. If the haematocrit is equal in artery and vein, then $K_1 = K_2 = K$. Thus the flow in the artery becomes:

Flow in artery during T_1 is

$$K \cdot N_a \cdot \frac{N_a + N_v}{N_a} \cdot V_{out} (+)$$

and

flow in vein during T_1 is

$$K \cdot N_v \cdot \frac{N_a + N_v}{N_v} \cdot V_{out} (-)$$

If the parts due to arterial and venous flow can be separated by visual or other means (e.g. suppose a constant flow in the vein, which has the value of $V_{out}(-)$ at the beginning of T_2) the foregoing is also true during T_2. This means that the output of the apparatus can be considered as being a flow, rather than a velocity, but one has to calibrate the outputs to obtain the value of $K \cdot (N_a + N_v)$.

b) The arterial bloodflow is positive during the whole cardiac cycle.

In this case separation of the doppler spectra corresponds with the separation of arterial and venous flow. The output of the adder (positive spectrum) must be processed in the same way as done in the old system to get V_{av} of the artery. Our system can easy be changed to do this. A phase shifting network (γ) and some switches should be added to cancel the 90° phase-shift introduced by the differentiation.

It is shown that in the majority of the probable occurring arterial and venous flows, the average value of the velocity can be calculated.

List of symbols.

Symbol	Description
ω_0	radial frequency of emitted signal.
c	velocity of ultrasound in blood.
v	velocity of particles or liquid.
$\Delta\omega$	radial frequency-shift.
$\mathcal{P}(\Delta\omega)$	power density spectrum.
$\Delta\omega_{max}$	highest radial frequency-shift.
$\Delta\omega_{min}$	lowest radial frequency-shift.
$\alpha\ (\beta)$	angle between velocity of the particle and emitter (receiver).
av	average.
$N,\ N_t$	total number of particles.
$N_{a+}\ (N_{a-})$	total number of particles in the artery, moving in the positive (negative) direction.
$N_{v+}\ (N_{v-})$	total number of particles in the vein, moving in the positive (negative) direction.
$V_{av\ a}$	average velocity of particles in the artery.
$V_{av+}\ (V_{av-})$	average velocity of all particles moving in the positive (negative) direction.
Δf_{av}	average frequency-shift.
$K_1,\ K_2,\ K$	constants.
ω_{min}	lowest radial frequency for which the phase shifting network gives a phase-shift of 45°.
ω_{max}	highest radial frequency for which the phase shifting network gives a phase-shift of 45°.

All other characters are explained or defined in the text or in the figures.

Appendix A.

Determination of the average frequency of the synchronous detected doppler spectrum by the system developed by ir. Arts (ref. 1).

Fig. 24 gives a simplified block diagram of the system. We shall consider the processing of a signal that contains just two sinusoidal components.

$$f(t) = A \cos\left\{(\omega_0 - \omega_{d1})t + \varphi_1\right\} + B \cos\left\{(\omega_0 + \omega_{d2})t + \varphi_2\right\}$$

The first term represents a negative frequency shift and the second term a positive one. After demodulation and bandpass filtering the two signals S_1 and S_2 are:

$$S_1 = \frac{A}{2} \sin\left(\omega_{d1}t - \varphi_1\right) - \frac{B}{2} \sin\left(\omega_{d2}t + \varphi_2\right)$$

$$S_2 = \frac{A}{2} \cos\left(\omega_{d1}t - \varphi_1\right) + \frac{B}{2} \cos\left(\omega_{d2}t + \varphi_2\right)$$

If differentiated and multiplied by S_2, the signal of the numerator becomes:

$$S_1' = \frac{A^2}{8} \cdot \omega_{d1}\left\{1 + \cos 2\left(\omega_{d1}t - \varphi_1\right)\right\} - \frac{B^2}{8}\omega_{d2}\left\{1 + \cos 2\left(\omega_{d2}t + \varphi_2\right)\right\} +$$
$$+ \frac{AB}{8}\left(\omega_{d1} - \omega_{d2}\right)\left\{\cos\left((\omega_{d2} + \omega_{d1})t + \varphi_2 - \varphi_1\right) +\right.$$
$$\left. + \cos\left((\omega_{d2} - \omega_{d1})t + \varphi_2 + \varphi_1\right)\right\}.$$

The quadratic form of S_2 is

$$S_2' = \frac{A^2}{8}\left\{1 + \cos 2\left(\omega_{d1}t - \varphi_1\right)\right\} + \frac{B^2}{8}\left\{1 + \cos 2\left(\omega_{d2}t + \varphi_2\right)\right\} +$$
$$+ \frac{AB}{4}\left\{\cos\left((\omega_{d1} + \omega_{d2})t - \varphi_1 + \varphi_2\right) +\right.$$
$$\left. + \cos\left((\omega_{d1} - \omega_{d2})t - \varphi_1 - \varphi_2\right)\right\}.$$

After lowpass filtering and division of numerator by denominator the output signal becomes:

$$V_{out} = -\frac{-A^2\omega_{d1} + B^2\omega_{d2}}{A^2 + B^2} \tag{18}$$

In the case of non-sinusoidal signals with a power density spectrum $\Phi(\omega)$, the fourier components can be treated likewise. This results in

$$V_{out} = - \frac{\sum\limits_{all\,\omega} A_i^2 \cdot \omega_i}{\sum\limits_{all\,\omega} A_i^2}$$

which corresponds to

$$V_{out} = - \frac{\int_{\Delta\omega_{min}}^{\Delta\omega_{max}} \Delta\omega \cdot \Phi(\Delta\omega) \cdot d(\Delta\omega)}{\int_{\Delta\omega_{min}}^{\Delta\omega_{max}} \Phi(\Delta\omega) \cdot d(\Delta\omega)} \qquad (19)$$

Remarks:

In the apparatus, the sign of V_{out} is changed. During the processing the sign of the direction of flow is saved, for ω_{d1} which has a negative sign (18) corresponds to a negative frequency-shift, which corresponds in its turn to flow of blood in the negative direction. V_{out} is independent of the total amount of energy, but depends merely on the shape of $\Phi(\omega)$.

Appendix B.

Calculation of a network that gives a phase shift of 45° in
the frequency range of 150-6000 hz (ref. 2).

The general expression for the transfer function of the
chosen network is:

$$H = H_o \prod_{k=1}^{n} \frac{1 + p_k \cdot p}{p + p_k}, \text{ where } H_o = \left| H(\omega_o) \right|,$$

$$p = \frac{j\omega}{\omega_o} \text{ and } \omega_o = \sqrt{\omega_{min} \cdot \omega_{max}}$$

The poles and zeros of the network are chosen in such a way
that to every pole $-p_K \omega_o$, a zero $-\omega_o/p_K$ corresponds.
It can simply be understood that the accuracy of the
desired phase-shift in the given frequency range is a
function of the number of terms in the expression of H. Our
choice of n=3 gives a maximum deviation of 20'. For $\omega = x\omega_o$
the transfer function changes into

$$H = H_o \frac{1 + j p_1 x}{jx + p_1} \cdot \frac{1 + j p_2 x}{jx + p_2} \cdot \frac{1 + j p_3 x}{jx + p_3} \tag{20}$$

The phase φ_K of each factor $1 + j p_K x/(jx + p_K)$ satisfies

$$\tan \varphi_K = \frac{p_K^2 - 1}{2 p_K} \cdot \frac{2x}{x^2 + 1}$$

If $\left(p_K^2 - 1 \right)/2 p_K = y_K$ and $\left(x^2 + 1 \right)/2x = y$ then the overall phase
shift satisfies

$$\tan \varphi = \tan (\varphi_1 + \varphi_2 + \varphi_3) = \frac{(y_1 + y_2 + y_3) y^2 - y_1 y_2 y_3}{y^3 - (y_1 y_2 + y_1 y_3 + y_2 y_3) y} = \frac{P_1 y^2 - P_3}{y^3 - P_2 y}$$

In the defined frequency range of 150-6000 hz the value of
the phase will vary slightly, thus

$$\tan \varphi_{min} \leqslant \frac{P_1 y^2 - P_3}{y^3 - P_2 y} \leqslant \tan \varphi_{max}$$

This can be rewritten as

$$1 \leqslant \frac{a_1 y^2 + a_3}{y^3 + a_2 y} = U_3 (Q, y) \leqslant \frac{\tan \varphi_{max}}{\tan \varphi_{min}} = Q$$

in which

$$a_1 = P_1 / \tan \varphi_{min} \quad , \quad a_2 = -P_2 \quad , \quad a_3 = -P_3 / \tan \varphi_{min} \tag{21}$$

The frequency range can be defined in y as follows:

$$\frac{\omega_{min}}{\omega_o} \leq x \leq \frac{\omega_{max}}{\omega_o} \quad \text{whereas} \quad y = \frac{x^2+1}{2x} \; ;$$

thus

$$1 \leq y \leq \frac{\omega_{max} + \omega_{min}}{2 \omega_o} = y_{max} \tag{22}$$

The problem is to find the proper value of a_1, a_2 and a_3. In reference 2 a solution is given with the aid of the parameter a:

$$y_{max} = a \sqrt{\frac{a(a+2)}{2a+1}} \qquad \text{in which} \quad a > 1 \tag{23}$$

$$Q = \frac{\tan \varphi_{max}}{\tan \varphi_{min}} = \frac{a+2}{2a+1} \sqrt{\frac{a(a+1)}{2a+1}} \tag{24}$$

$$U_3(Q,y) = \frac{\tan \varphi_{max}}{\tan \varphi_{min}} \cdot \frac{(2a+1)y^2 + a^2}{y^3 + a(a+2)y} \tag{25}$$

With the aid of the theoretical background the numerical solution can be found in the following way:

a) ω_{max} and $\omega_{min} \longrightarrow y_{max}$

b) $y_{max} \longrightarrow a$ by eq. (23)

c) $a \longrightarrow Q$. By linearisation of $\tan \varphi$ around $\varphi = 45°$, the value of $\tan \varphi_{min}$ and $\tan \varphi_{max}$ can be found.

d) a, $Q \longrightarrow a_1$, a_2, a_3 by eq. (25).

e) a_1, a_2, a_3, $\tan \varphi_{min} \longrightarrow P_1$, P_2, P_3 by eq. (21).

f) P_1, P_2, $P_3 \longrightarrow y_1$, y_2, y_3. The values of y_1, y_2 and y_3 are found as the roots of equation
$$y^3 - P_1 y^2 + P_2 y - P_3 = 0 .$$

g) y_1, y_2, $y_3 \longrightarrow p_1$, p_2, p_3 by $p_K = y_K + \sqrt{y_K^2 + 1}.$

This all gives us three poles and zeros; namely

a pole $\longrightarrow$ $-p_K \omega_o$

a zero $\longrightarrow$ $-\omega_o/p_K$ in which K = 1,2,3.

The numerical treatment is done by digital computer. Fig. 25 gives the solution of $U_3(Q,y)$ and the values of the poles and zeros are:

poles: $.243512866 \cdot 10^{-2}$
            $.259164010 \cdot 10^{-3}$
            $.434642086 \cdot 10^{-4}$

zeros: $.115578178 \cdot 10^{-4}$
            $.108598309 \cdot 10^{-3}$
            $.647539071 \cdot 10^{-3}$

References.

1. Arts, M.G.J.,
   On the instantaneous measurement of bloodflow by ultra-
   sonic means.
   T.H. Report 71-E-20.

2. Zaalberg van Zelst, J.J.,
   De berekening van impedanties, waarvan de phasehoek in
   een gegeven frequentiegebied tussen voorgeschreven waarden
   ligt.
   Nat.Lab. Rapport nr. 83/61.

3. Weys, G.J.M.,
   Doppler flow meting door bepaling van gemiddelde
   frequentie. Instrumentatie en testmethoden.
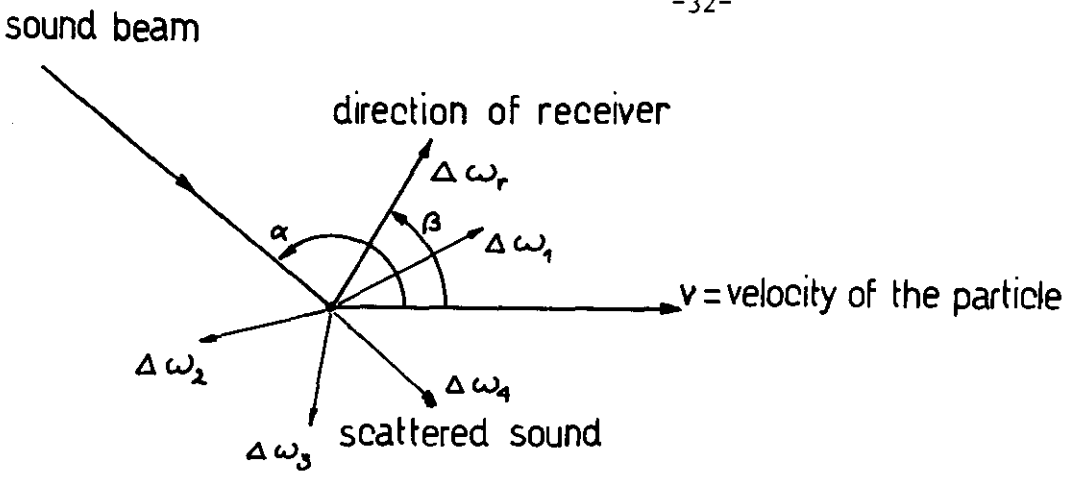
fig. 1
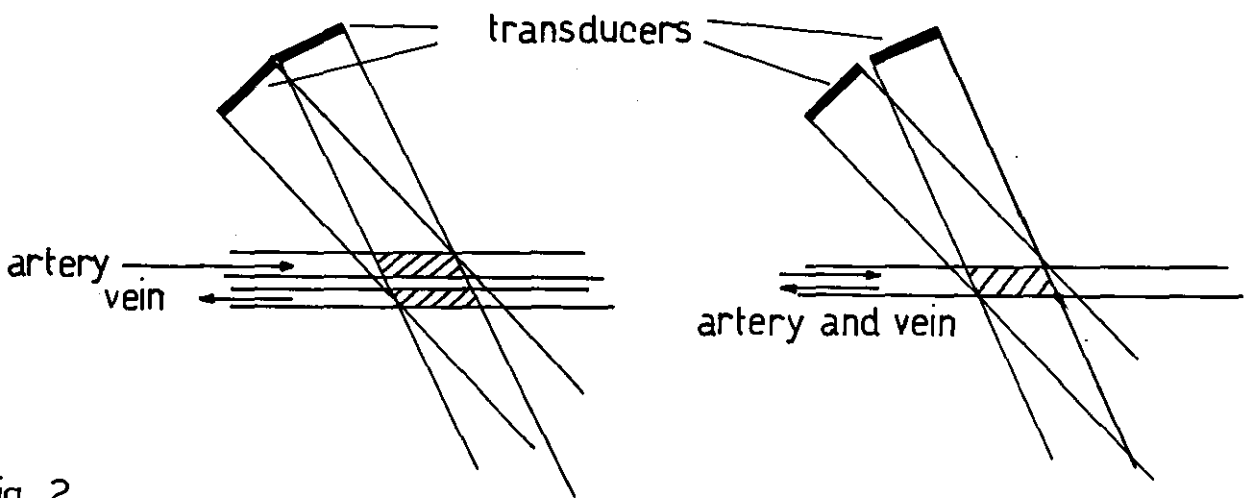
fig. 2
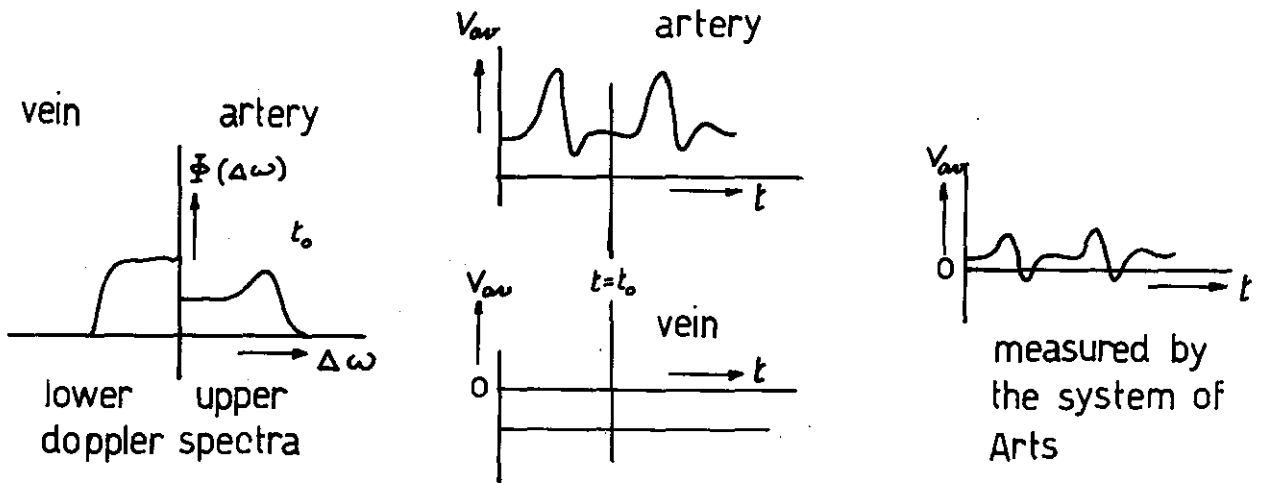
fig. 3
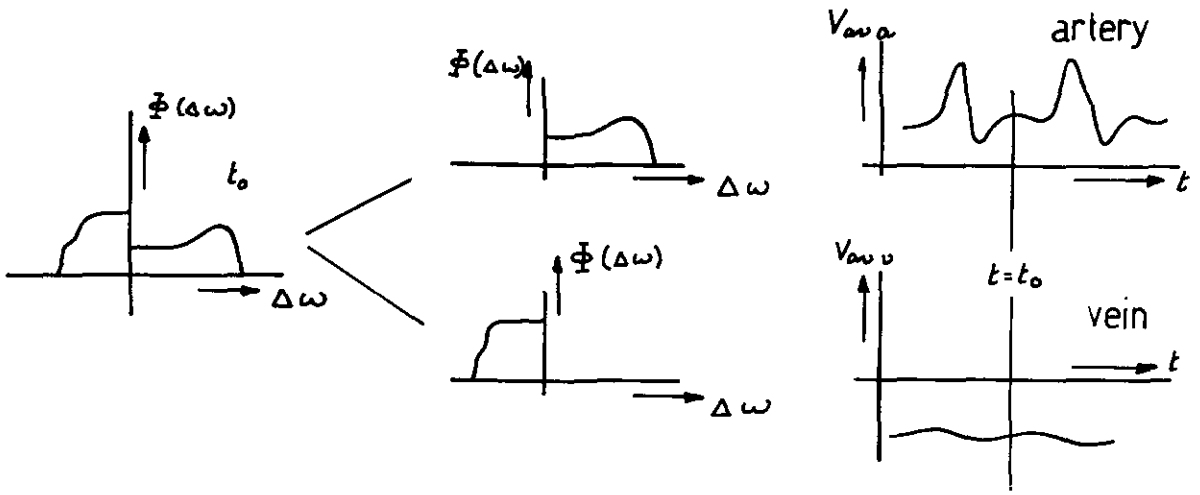
fig. 4
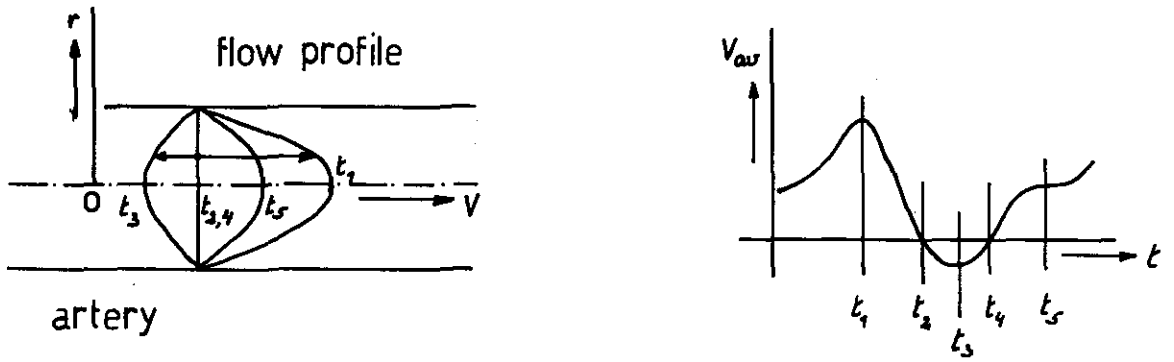
fig. 5
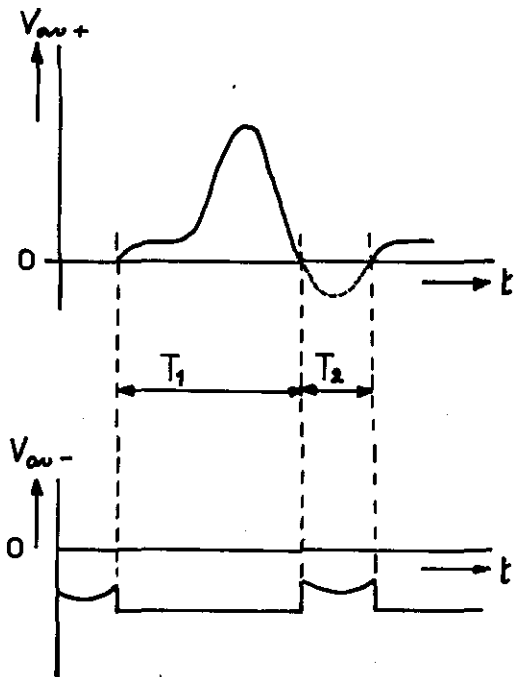
fig. 6
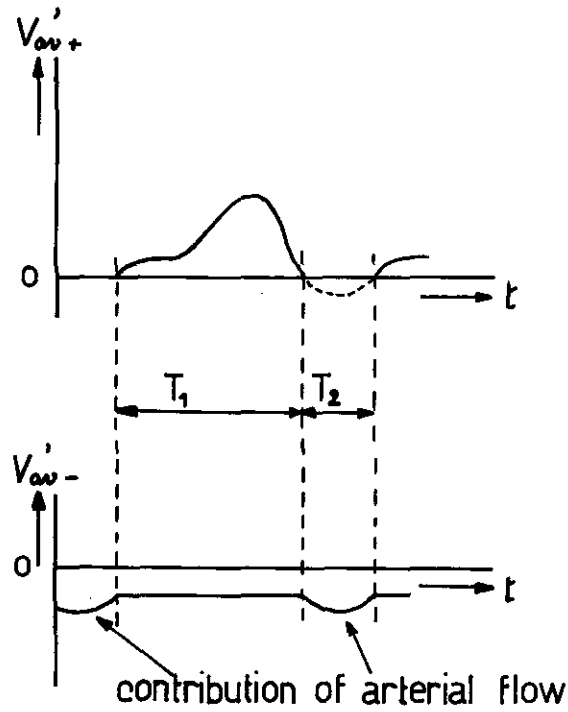
fig. 7
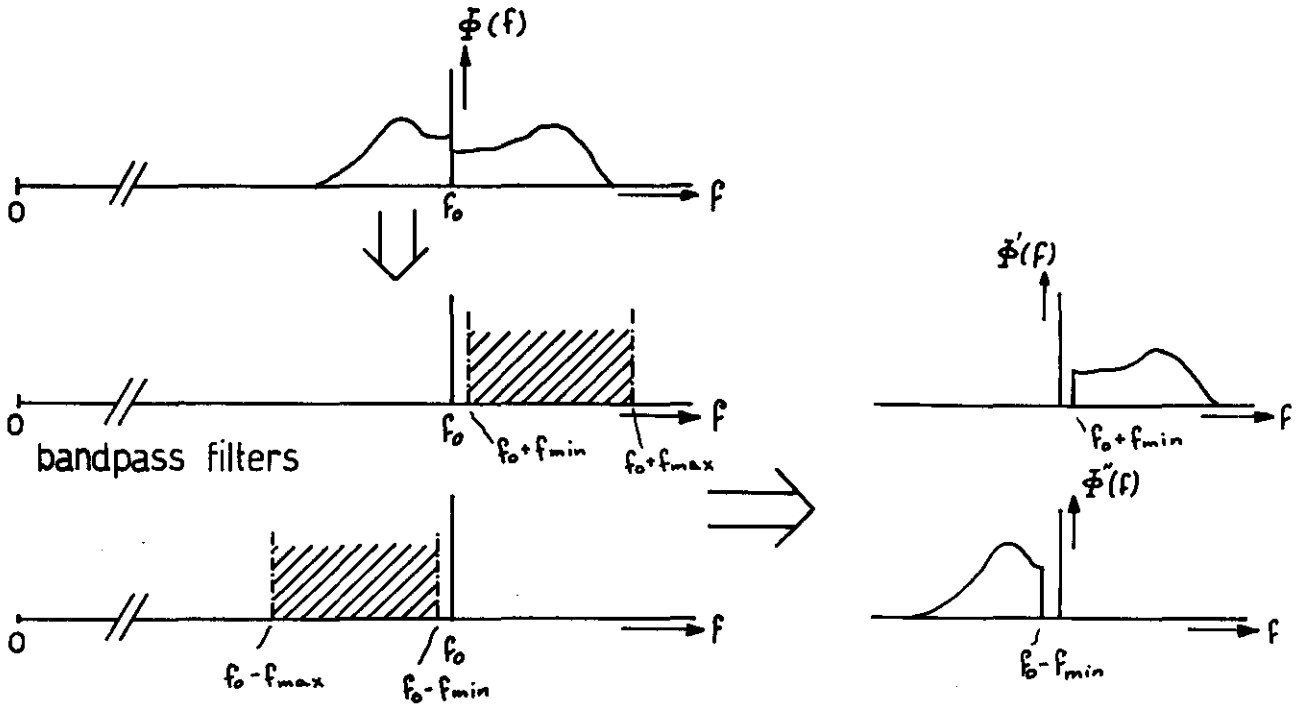
fig. 8a
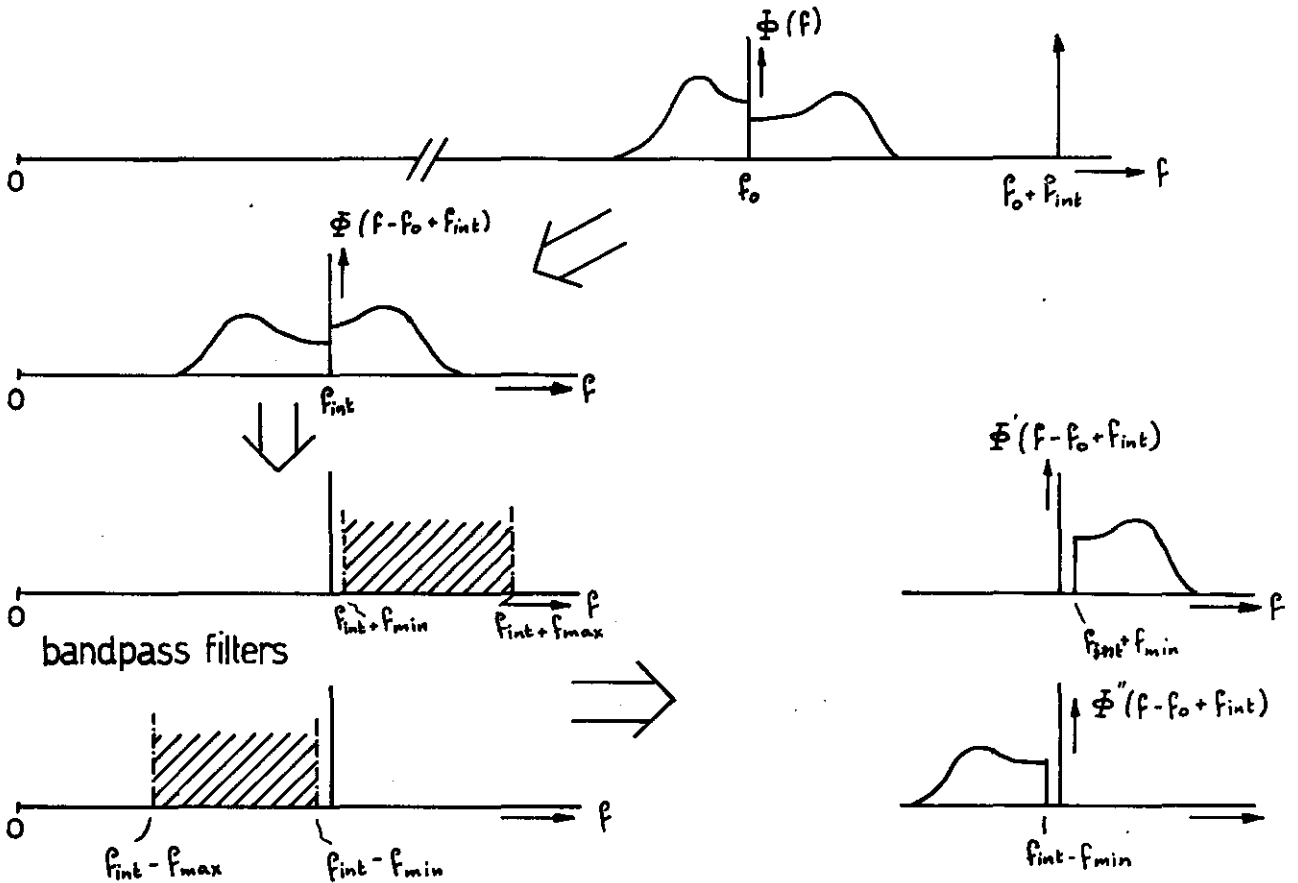
fig. 8b
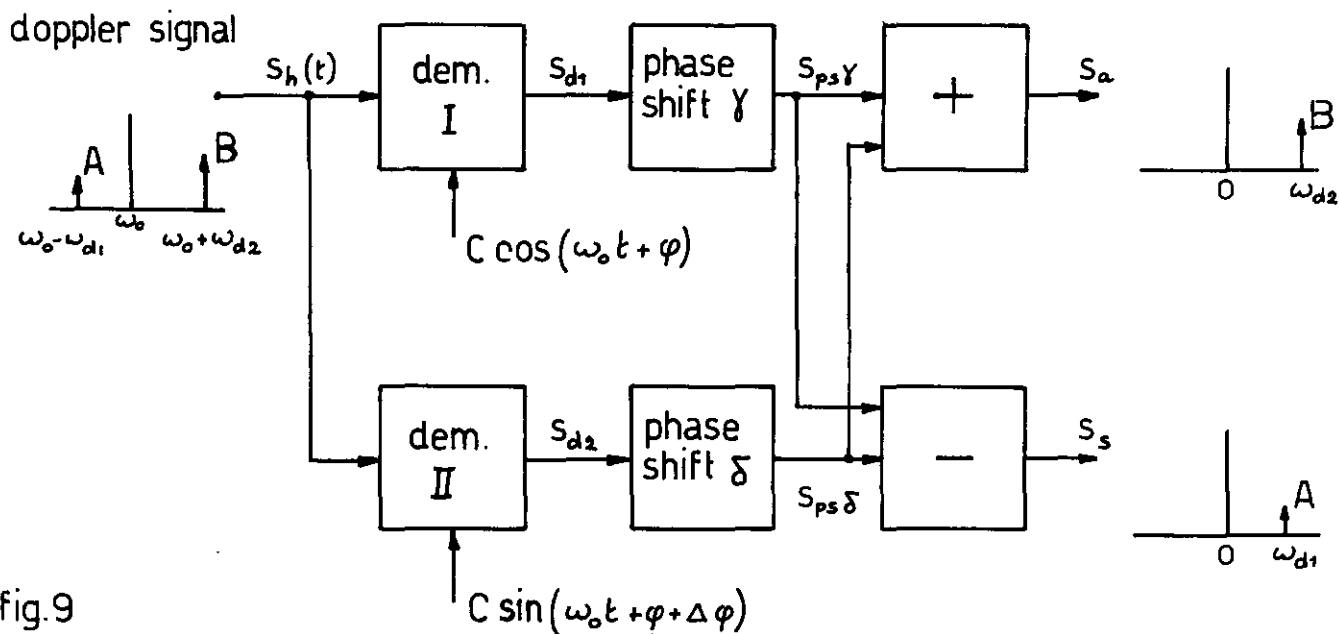
fig. 9
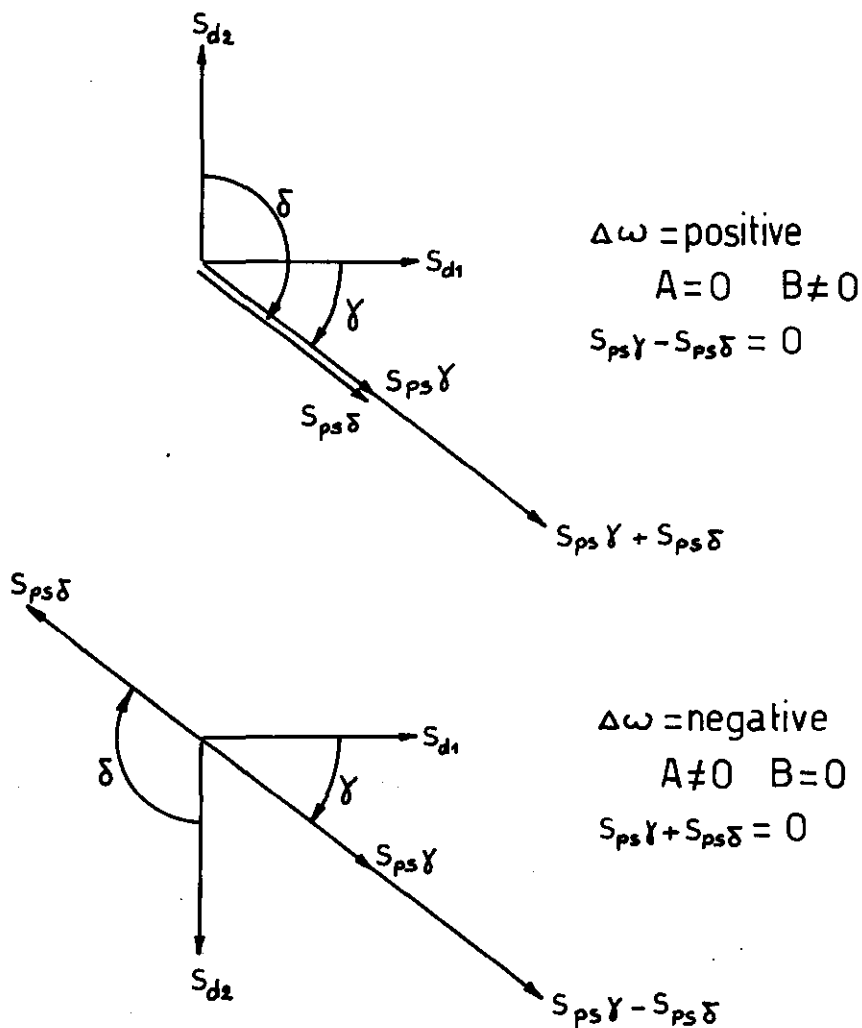
fig. 10
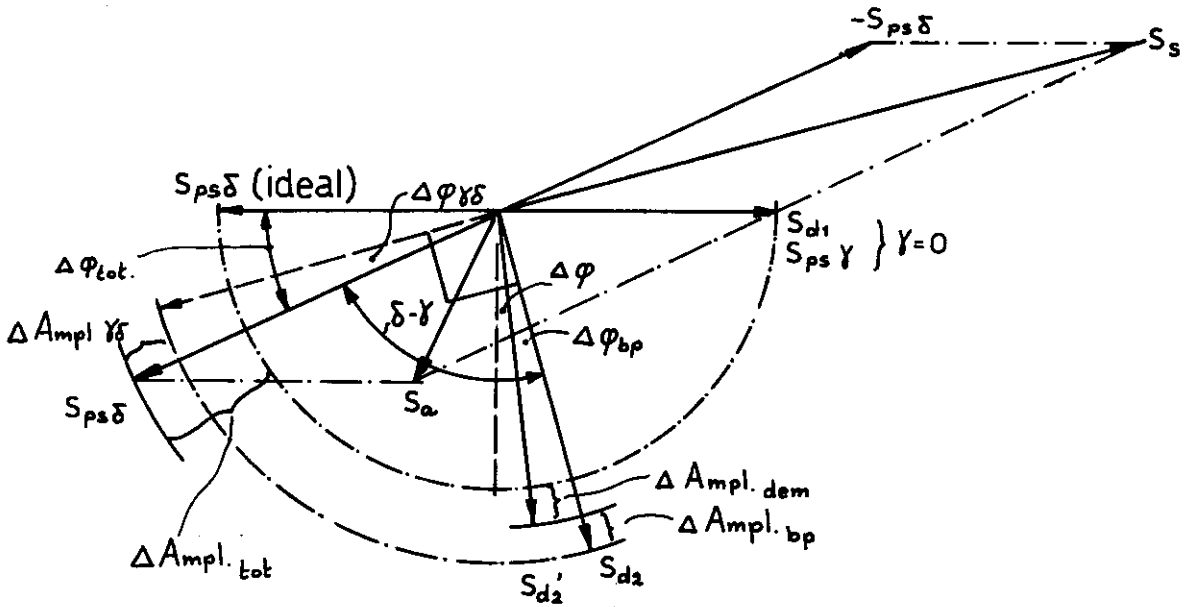
$$\Delta\varphi = \text{error in phase-shift caused by demodulation}$$
$$\Delta\varphi_{bp} = \text{"} \quad \text{"} \quad \text{"} \quad \text{"} \quad \text{"} \quad \text{bandpass filtering}$$
$$\Delta\varphi_{\gamma\delta} = \text{"} \quad \text{"} \quad \text{"} \quad \text{"} \quad \text{"} \quad \text{phase-shift } \gamma \text{ and } \delta$$

$$\Delta\text{Ampl.}_{dem.} = \text{error in amplitude caused by demodulation}$$
$$\Delta\text{Ampl.}_{bp} = \text{"} \quad \text{"} \quad \text{"} \quad \text{"} \quad \text{"} \quad \text{bandpass filtering}$$
$$\Delta\text{Ampl.}_{\gamma\delta} = \text{"} \quad \text{"} \quad \text{"} \quad \text{"} \quad \text{"} \quad \text{phase-shift } \gamma \text{ and } \delta$$

fig. 11

fig.12

fig. 13

fig. 14

(a)   (b)

fig. 15

generator transducers hf amplifier demodulators bandpass filters phase shifting networks adders

R & S

L 103

MC 1596

2× μA709 S_{d1}

γ

μA709 S_a

→ flow

δ S_K

phase-shift

R-C

MC 1596

2× μA709

δ

μA709 S_s

demodulating part of the system

-39-

multipliers   dividers

differentiators   lowpass filters

positive spectrum S_a → μA709 S_{dp} → MC 1596 $S_{dp}× S_K$ → R-C N(+) → MC 1596 → V_{out} (+)

spectrum of denominator S_K → S_K → MC 1596 S_K^2 → R-C D

negative spectrum S_s → μA709 → MC 1596 → R-C N(−) → MC 1596 → V_{out} (−)
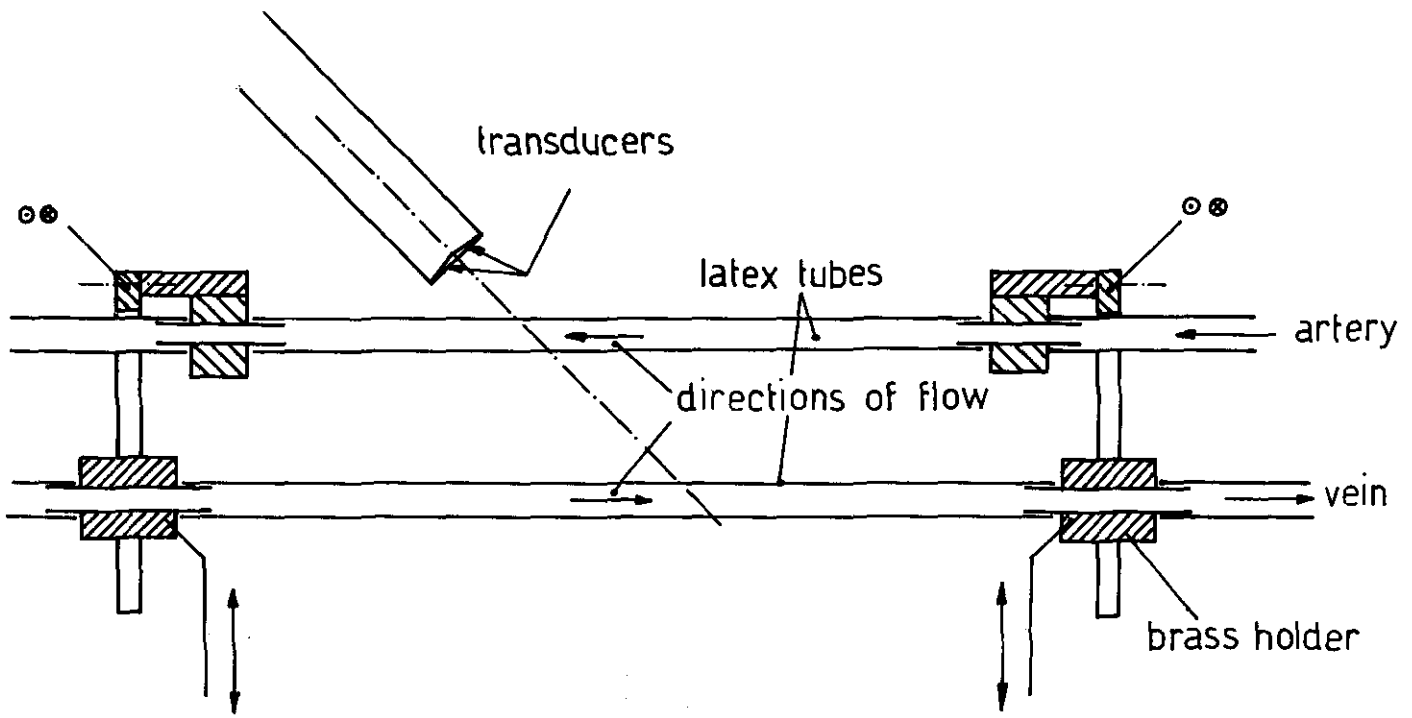
fig. 16

processing part of the system

fig. 17
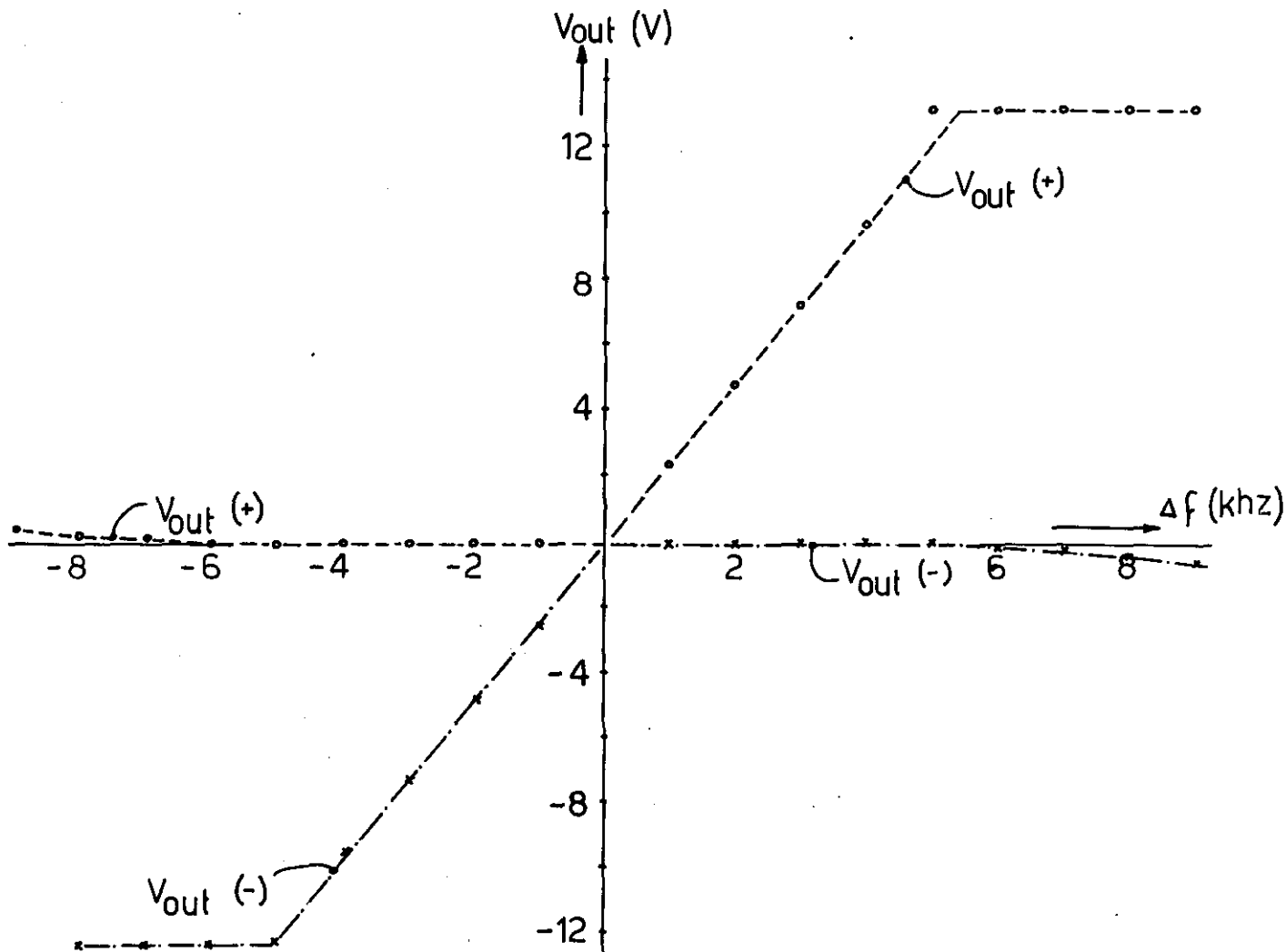
fig. 18
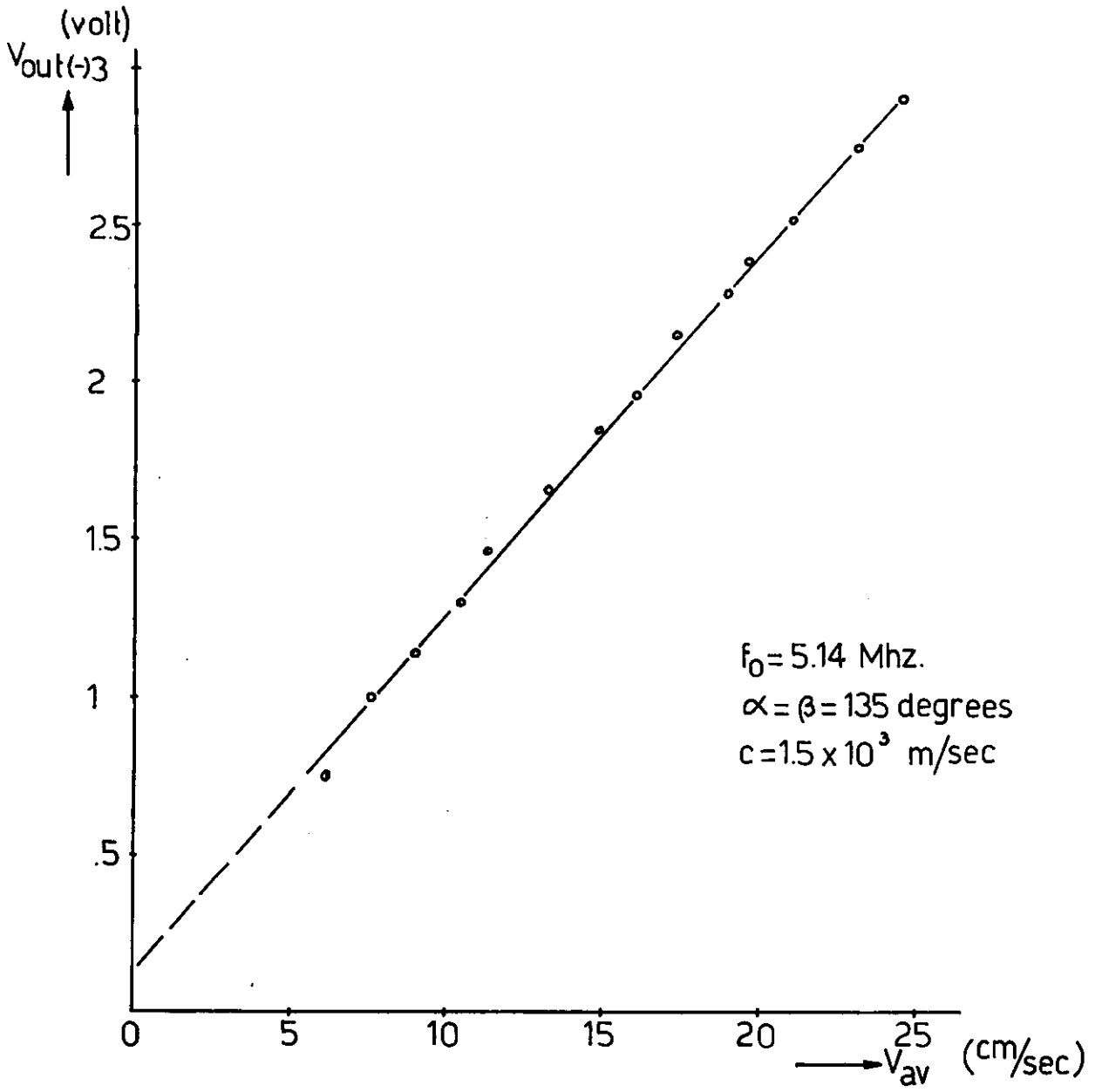
fig. 19

cm/sec

doppler „positive channel"

cc/sec

transflow 600

fig. 20

cm/sec

fig. 21   doppler „both channels"

cc/sec

fig. 22   doppler

timescales .5 sec/cm

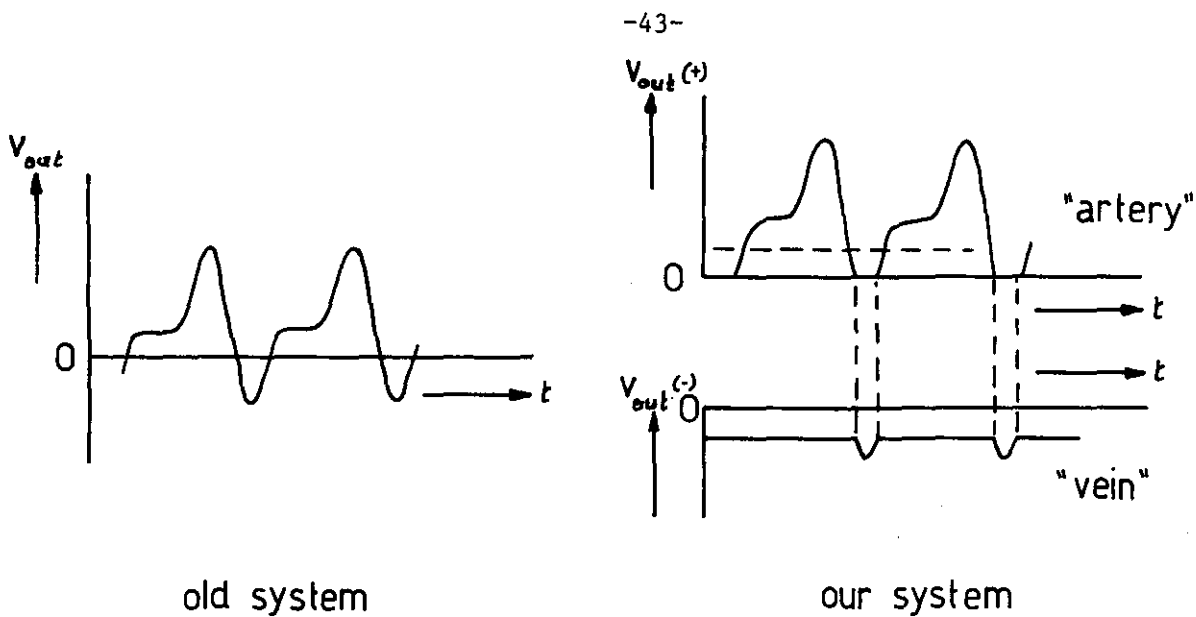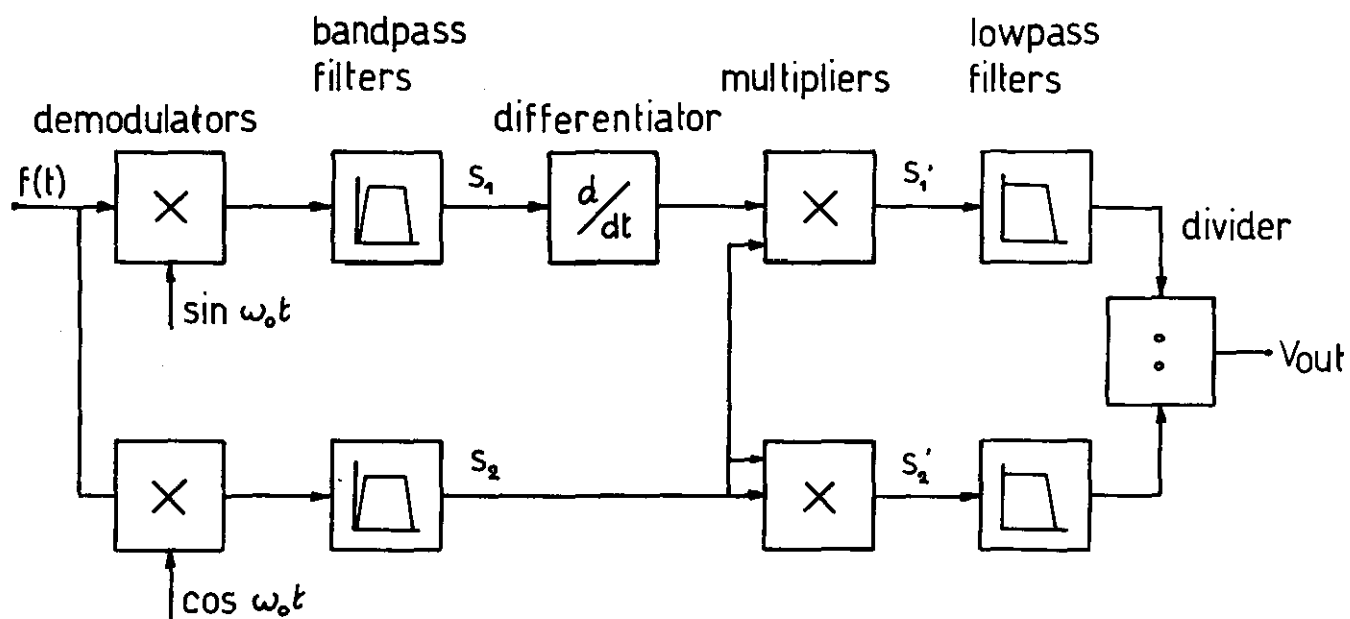old system   our system
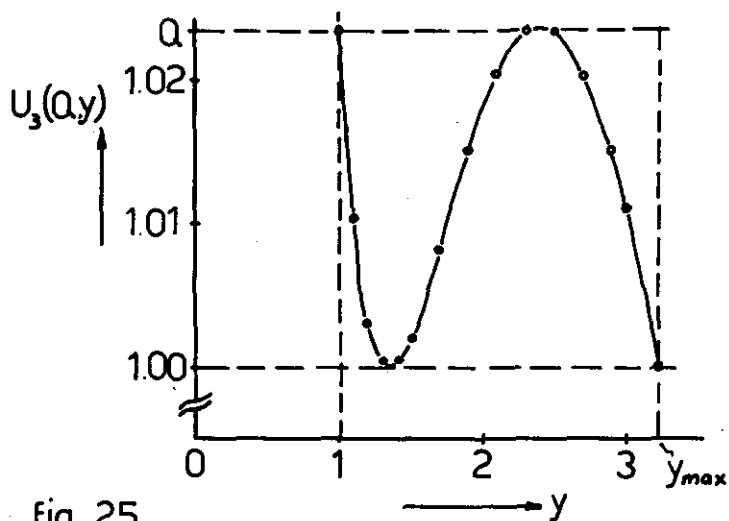
fig. 23

fig. 24

fig. 25

EINDHOVEN UNIVERSITY OF TECHNOLOGY

THE NETHERLANDS

DEPARTMENT OF ELECTRICAL ENGINEERING

TH-Reports:

1. Dijk, J., M. Jeuken and E.J. Maanders
   AN ANTENNA FOR A SATELLITE COMMUNICATION GROUND STATION (PROVISIONAL ELEC-
   TRICAL DESIGN). TH-report 60-E-01. March 1968. ISBN 90 6144 001 7.

2. Veefkind, A., J.H. Blom and L.H.Th. Rietjens.
   THEORETICAL AND EXPERIMENTAL INVESTIGATION OF A NON-EQUILIBRIUM PLASMA
   IN A MHD CHANNEL. TH-report 68-E-2. March 1968. ISBN 90 6144 002 5.
   Submitted to the Symposium on a Magnetohydrodynamic Electrical Power Ge-
   neration, Warsaw, Poland, 24-30 July, 1968.

3. Boom, A.J.W. van den and J.H.A.M. Melis.
   A COMPARISON OF SOME PROCESS PARAMETER ESTIMATING SCHEMES.
   TH-report 68-E-03. September 1968. ISBN 90 6144 003 3.

4. Eykhoff, P., P.J.M. Ophey, J. Severs and J.O.M. Oome.
   AN ELECTROLYTIC TANK FOR INSTRUCTIONAL PURPOSES REPRESENTING THE COMPLEX-
   FREQUENCY PLANE. TH-report 68-E-04. September 1968. ISBN 90 6144 004 1.

5. Vermij, L. and J.E. Daalder.
   ENERGY BALANCE OF FUSING SILVER WIRES SURROUNDED BY AIR.
   TH-report 68-E-05. November 1968. ISBN 90 6144 005 X.

6. Houben, J.W.M.A. and P. Massee.
   MHD POWER CONVERSION EMPLOYING LIQUID METALS.
   TH-Report 69-E-06. February 1969. ISBN 90 6144 006 8.

7. Heuvel, W.M.C. van den and W.F.J. Kersten.
   VOLTAGE MEASUREMENT IN CURRENT ZERO INVESTIGATIONS.
   TH-Report 69-E-07. September 1969. ISBN 90 6144 007 6.

8. Vermij, L.
   SELECTED BIBLIOGRAPHY OF FUSES.
   TH-Report 69-E-08. September 1969. ISBN 90 6144 008 4.

9. Westenberg, J.Z.
   SOME IDENTIFICATION SCHEMES FOR NON-LINEAR NOISY PROCESSES.
   TH-Report 69-E-09. December 1969. ISBN 90 6144 009 2.

10. Koop, H.E.M., J. Dijk and E.J. Maanders.
    ON CONICAL HORN ANTENNAS.
    TH-Report 70-E-10, February 1970. ISBN 90 6144 010 6.

11. Veefkind, A.
    NON-EQUILIBRIUM PHENOMENA IN A DISC-SHAPED MAGNETOHYDRODYNAMIC GENERATOR.
    TH-Report 70-E-11. March 1970. ISBN 90 6144 011 4.

12. Jansen, J.K.M., M.E.J. Jeuken and C.W. Lambrechtse.
    THE SCALAR FEED.
    TH-Report 70-E-12. December 1969. ISBN 90 6144 012 2

13. Teuling, D.J.A.
    ELECTRONIC IMAGE MOTION COMPENSATION IN A PORTABLE TELEVISION CAMERA.
    TH-Report 70-E-13. 1970. ISBN 90 6144 013 0.

14. Lorencin, M.
    AUTOMATIC METEOR REFLECTIONS RECORDING EQUIPMENT.
    TH-Report 70-E-14. November 1970. ISBN 90 6144 014 9.

15. Smets, A.J.
    THE INSTRUMENTAL VARIABLE METHOD AND RELATED IDENTIFICATION SCHEMES.
    TH-Report 70-E-15. November 1970. ISBN 90 6144 015 7.

16. White, Jr., R.C.
    A SURVEY OF RANDOM METHODS FOR PARAMETER OPTIMIZATION.
    TH-Report 70-E-16. February 1971. ISBN 90 6144 016 5.

17. Talmon, J.L.
    APPROXIMATED GAUSS-MARKOV ESTIMATORS AND RELATED SCHEMES.
    TH-Report 71-E-17. February 1971. ISBN 90 6144 017 3.

18. Kalásek, V.
    MEASUREMENT OF TIME CONSTANTS ON CASCADE D.C. ARC IN NITROGEN.
    TH-Report 71-E-18. February 1971. ISBN 90 6144 018 1.

19. Hosselet, L.M.L.F.
    OZONBILDUNG MITTELS ELEKTRISCHER ENTLADUNGEN.
    TH-Report 71-E-19. March 1971. ISBN 90 6144 019 X.

20. Arts, M.G.J.
    ON THE INSTANTANEOUS MEASUREMENT OF BLOODFLOW BY ULTRASONIC MEANS.
    TH-Report 71-E-20. May 1971. ISBN 90 6144 020 3.

21. Roer, Th. G. van de
    NON-ISO THERMAL ANALYSIS OF CARRIER WAVES IN A SEMICONDUCTOR.
    TH-Report 71-E-21. August 1971. ISBN 90 6144 021 1.

22. Jeuken, P.J., C. Huber and C.E. Mulders.
    SENSING INERTIAL ROTATION WITH TUNING FORKS.
    TH-Report 71-E-22. September 1971. ISBN 90 6144 022 X.

23. Dijk, J. and E.J. Maanders.
    APERTURE BLOCKING IN CASSEGRAIN ANTENNA SYSTEMS. A REVIEW.
    TH-Report 71-E-23. September 1971. ISBN 90 6144 023 8 (in preparation.

24. Kregting, J. and R.C. White, Jr.
    ADAPTIVE RANDOM SEARCH.
    TH-Report 71-E-24. October 1971. ISBN 90 6144 024 6 (in preparation).

25. Damen, A.A.H. and H.A.L. Piceni.
    TH-Report 71-E-25. October 1971. ISBN 90 6144 025 4 (in preparation).

26. Bremmer, H.
    A MATHEMATICAL THEORY CONNECTING SCATTERING AND DIFFRACTION PHENOMENA'
    INCLUDING BRAGG-TYPE INTERFERENCES.
    TH-Report 71-E-26. December 1971. ISBN 90 6144 026 2.

27. Bokhoven, W.M.G. van
    METHODS AND ASPECTS OF ACTIVE-RC FILTERS SYNTHESIS.
    TH-Report 71-E-27. 10 December 1970. ISBN 90 6144 027 0.

28. Boeschoten, F.
    TWO FLUIDS MODEL REEXAMINED.
    TH-Report 72-E-28. March 1972. ISBN 90 6144 028 9.

29. Rietjens, L.H.Th.
    REPORT ON THE CLOSED CYCLE MHD SPECIALIST MEETING. WORKING GROUP OF THE
    JOINT ENEA: IAEA INTERNATIONAL MHD LIAISON GROUP AT EINDHOVEN, THE NETHER-
    LANDS. September 20, 21 and 22, 1971.
    TH-Report 72-E-29. April 1972. ISBN 90 6144 029 7

30. C.G.M. van Kessel and J.W.M.A. Houben.
    LOSS MECHANISMS IN AN MHD-GENERATOR.
    TH-Report 72-E-30. June 1972. ISBN 90 6144 030 0.

31. A. Veefkind.
    CONDUCTING GUIDS TO STABILIZE MHD-GENERATOR PLASMAS AGAINST IONIZATION
    INSTABILITIES. TH-Report 72-E-31. October 1972. ISBN 90 6144 031 9.

32. J.E. Daalder and C.W.M. Vos.
    DISTRIBUTION FUNCTIONS OF THE SPOT-DIAMETER FOR SINGLE- AND MULTI-CATHODE
    DISCHARGES IN VACUUM. TH-Report 73-E-32. January 1973. ISBN 90 6144 032 7.

33. J.E. Daalder.
    JOULE HEATING AND DIAMETER OF THE CATHODE SPOT IN A VACUUM ARC.
    TH-Report 73-E-33. January 1973. ISBN 90 6144 033 5.

34. Huber, C.
    BEHAVIOUR OF THE SPINNING GYRO ROTOR.
    TH-Report 73-E-34. February 1973. ISBN 90 6144 034 3.

35. Boeschoten, F.
    THE VACUUM ARC AS A FACILITY FOR RELEVANT EXPERIMENTS IN FUSION
    RESEARCH.
    TH-Report 73-E-35, February 1973, ISBN 90 6144 035 1.

36. Blom, J.A.
    ANALYSIS OF PHYSIOLOGICAL SYSTEMS BY PARAMETER ESTIMATION TECHNIQUES.
    73-E-36. 1973. ISBN 90 6144 036 X

37. Lier, M.C. van and R.H.J.M. Otten.
    AUTOMATIC WIRING DESIGN.
    TH-reprot 73-E-37. May 1973. ISBN 90 6144 037 8

38. Andriessen, F.J.
    CALCULATION OF RADIATION LOSSES IN CYLINDRICAL SYMMETERICAL HIGH
    PRESSURE DISCHARGES BY MEANS OF A DIGITAL COMPUTER.
    TH-report 73-E-38. October 1973. ISBN 90 6144 038 6

39. Dijk, J., C.T.W. van Diepenbeek, E.J. Maanders and L.F.G. Thurlings.
    THE POLARIZATION LOSSES OF OFFSET ANTENNAS.
    TH-report 73-E-39. June 1973. ISBN 90 6144 039 4.